June 18, 2024

Final Scientific Report for the KAT6 Foundation

Mitochondrial respiration and glycolysis analyses of dermal fibroblasts from KAT6A patients and healthy individuals using Seahorse XFe96 Analyzer

Prof. Yehuda G. Assaraf

The Fred Wyszkowki Cancer Research Lab,

Faculty of Biology, Technion-Israel Institute of Technology,

Haifa 3200003, Israel

Introduction

The process of glycolysis results in the release of protons into the extracellular medium causing acidification of the medium. Oxygen Consumption Rate (OCR) indicates mitochondrial function since ATP synthesis is coupled to oxygen consumption. OCR and extracellular acidification rate (ECAR) were measured in human adherent dermal fibroblasts using the Agilent Seahorse XFe96 Analyzer along with the Cell Mito Stress Test assay or Glycolysis Stress Test assay (Divakaruni et al., 2014). These measurements indicate the mitochondrial respiration and glycolytic function of the cells and together can report on the cellular bioenergetic function of KAT6A patient's fibroblasts compared with fibroblasts from healthy individuals. Impaired mitochondrial function affects tissues with high energy demand such as skeletal muscle and brain and can result in abnormal muscle tone, ataxia, seizures, impaired vision and hearing, developmental delays, and

respiratory problems, some of which appeared as symptoms in KAT6A patients (Russell et al., 2020; Wiesel-Motiuk and Assaraf, 2020).

Cell Mito Stress Test assay enable measuring mitochondrial function and provides insights into the cause of mitochondrial dysfunction. The sequential addition of ATP synthase inhibitor oligomycin, electron transport chain uncoupler FCCP and complex I and III inhibitors rotenone and antimycin A, respectively, enables the measurement of various parameters of respiratory function (Figure 2a). These parameters include: basal respiration (basal measurement minus non-mitochondrial respiration), maximal respiration (maximum OCR after FCCP response minus non-mitochondrial respiration), spare respiratory capacity (maximum OCR minus basal mitochondrial OCR) and proton leak (minimum rate after oligomycin response minus non-mitochondrial respiration) (Figure 2a).

Glycolysis Stress Test assay enables measuring glycolytic function by determining extracellular acidification rate under basal conditions and after the sequential addition of glucose, oligomycin and the non-metabolizable glucose analogue 2-deoxy-D-glucose (2-DG), which inhibits glycolysis. This assay enables calculation of glycolysis (maximum ECAR before oligomycin response minus ECAR before glucose injection), glycolytic capacity (maximum ECAR after oligomycin response minus ECAR before glucose injection) and glycolytic reserve (glycolytic capacity minus glycolysis) (Figure 4a).

Results and conclusions

The number of fibroblast cells seeded was optimized for the various experiments. 10,000 cells/well resulted in a higher OCR than 15,000 cells/well and were therefore determined as the optimal number of cells to be seeded (Figure 1a). The concentration of FCCP was also

optimized. Cells were treated with 1, 2, 2.5 and 3 μM FCCP and the optimal concentration was determined to be 2.5 μM (Figure 1b).

Mitochondrial respiration and glycolysis test analyses were performed in order to compare the bioenergetic status of KAT6A patients derived fibroblasts and two wild-type control fibroblasts derived from healthy individuals. The overall respiratory responses of patient-derived and control fibroblasts are shown in Figure 2b. This analysis revealed that the basal respiration is different between the fibroblast samples: control 2 (CTR2) fibroblasts displayed a markedly higher OCR, whereas patient derived (KAT6AF-P) fibroblasts had slightly higher OCR than control 1 (CTR1) fibroblasts. Spare respiratory capacity could not be determined since the maximal respiration was not higher than the basal respiration. This might be the result of cells being in their maximal respiration capacity before the addition of oligomycin.

Since the two control fibroblast cells showed different and opposed basal respiration rates compared to the KAT6A-patient derived fibroblasts, one cannot make conclusions regarding mitochondrial function of KAT6A-patient derived fibroblasts and the experiment was repeated twice with CTR3 control cells instead of CTR2 cells. In contrast to the previous experiment, KAT6AF-P1 fibroblasts had the highest basal respiration compared to control cells. Overall, there was a significant difference in basal respiration between all the cells, while CTR3 fibroblasts had markedly higher basal respiration compared to CTR1 (Figure 2c).

Galactose (GAL)-containing medium, instead of glucose (GLU), is known to shift energy metabolism towards mitochondrial respiration (Hertig et al., 2019). Cells grown in galactose-containing medium are thus characterized by a decreased glycolytic rate and an increased mitochondrial oxidative phosphorylation capacity. In this respect, cells with mitochondrial defects might not be able to increase their aerobic metabolism, i.e., elevation of OCR. A

preliminary experiment showed that galactose-containing medium increased the OCR of CTR1 cells. Two Mito Stress Test experiments were performed comparing OCR between KAT6AF-P1, CTR1 and CTR3 fibroblast cells in GLU or GAL-containing medium to compare mitochondrial function of KAT6A patient's cells and control cells. GAL medium increased the OCR of both control cells and the KAT6A patient cells (Figure 3a). Similar to the results of GLU-containing medium, KAT6AF-P1 fibroblasts had the highest basal OCR in GAL-containing medium (Figure 3b), and did not exhibit indications of mitochondrial defects.

ECAR measurements (Figure 4b) revealed that KAT6AF-P1 fibroblasts had higher glycolysis rate and glycolytic capacity than CTR1 and CTR2.

Mitochondrial respiration test analyses were repeated with a larger sample size of four patient-derived fibroblast cells (P1-P4) as well as four control-derived fibroblast cells (CTR1-CTR4) (Figure 5a-h). Analysis of the results showed that there was an extensive variability in basal respiration (5c-d) and maximal respiration (5e-f) of fibroblast samples and there was no segregation between the groups of patient-derived cells and healthy control-derived cells. Spare respiratory capacity (5g-h) could not be determined for all samples since the maximal respiration was not higher than the basal respiration for all cell samples. Overall, the control-derived cell group did not have higher spare respiratory capacity than KAT6A patient-derived cell group.

Taken together, the above results suggest that KAT6A patient-derived fibroblasts do not exhibit impaired mitochondrial respiration or glycolysis. It is possible that KAT6A affects cellular bioenergetic function in higher energy demanding cells (like neurons and muscle cells) or in cells undergoing metabolic reprograming.

In the latter respect, we undertook CRISPR Cas9 knockout of the KAT6A gene in human neuroblastoma SH-SY5Y cells which serve as neuronal cell model in various studies. OCR and ECAR were also measured in human neuroblastoma SH-SY5Y WT cells and SH-SY5Y KAT6A knockout (KO) cells. The number of SH-SY5Y cells and FCCP concentration were optimized for the experiments (Figure 6). 7,000 cells/well resulted in similar OCR to 10,000 cells/well but the OCR was too high (>100 pmol/min). Hence, 4,000 cells/well were seeded in the following experiments. Cells were treated with a range of 0.3-4 μM FCCP and the optimal concentration was determined to be 3.5-4μM (Figure 6b).

Mitochondrial respiration analysis was performed with SH-SY5Y WT cells as well as SH-SY5Y KAT6A KO cells. The overall respiratory responses of the cells are shown in Figure 7(a,b). SH-SY5Y KAT6A KO cells had slightly higher basal respiration than WT cells in the first experiment (after normalization to protein amount) (Figure 7a) and similar in the second experiment (Figure 7b).

ECAR measurements (Figure 8) revealed that SH-SY5Y WT cells had higher glycolysis rate than SH-SY5Y KAT6A KO cells. The ratio of basal glycolysis rate between SH-SY5Y KAT6A KO cells and SH-SY5Y WT cells was ~67%. *The difference in glycolysis rate between SH-SY5Y KAT6A KO cells and SH-SY5Y WT cells suggests that KAT6A has a direct or indirect role in glycolysis in SH-SY5Y cells.*

KAT6A plays a key role in regulation of gene expression via modification of histone lysine residues that modulate chromatin organization, hence can modulate the expression of many genes including genes encoding glycolytic proteins. Real-time qPCR analysis was performed in order to determine the mRNA levels of glycolytic genes in SH-SY5Y WT cells and SH-SY5Y KAT6A KO cells. Relative HK2 mRNA levels in SH-SY5Y KAT6A KO cells was lower than in

WT cells (75%) (Figure 9), suggesting that KAT6A might affect HK2 expression directly or indirectly. Hexokinase 2 is an isoform of hexokinase enzyme which in humans is encoded by the *HK2* gene. Hexokinases phosphorylate glucose to produce glucose-6-phosphate (G6P), the first step in glucose metabolism pathways. The expression levels of other glycolytic genes (PGK1, PKM and LDHA) were similar in WT and KAT6A KO cells (Figure 9).

These interesting results suggest that KAT6A may affect glycolysis in some cell types. Recently, Fu et al., (Fu et al., 2024) showed that KAT6A regulated glycolytic gene expression and glucose metabolic reprogramming in mouse $CD4^+$ T cells. Specifically, KAT6A supported the proliferation and differentiation of a subset of $CD4^+$ specific T cells associated with autoimmunity. KAT6A deficiency led to downregulation of cell cycle and glycolytic gene expression and to diminished histone acetylation marks H3K9 and H3K27 at the promoter and transcriptional regions of glycolytic genes. Glycolytic measurements revealed that glycolytic function was decreased in KAT6A-deficient $CD4^+$ T cells following antigen stimulation, but not in resting T cells. In contrast, mitochondrial respiration measurements were comparable in KAT6A-deficient $CD4^+$ T cells both under resting and stimulated conditions.

We conclude that patient-derived fibroblasts may not be the first model of choice for the study of mitochondrial respiration and glycolytic function in KAT6A mutant cells.

Figures

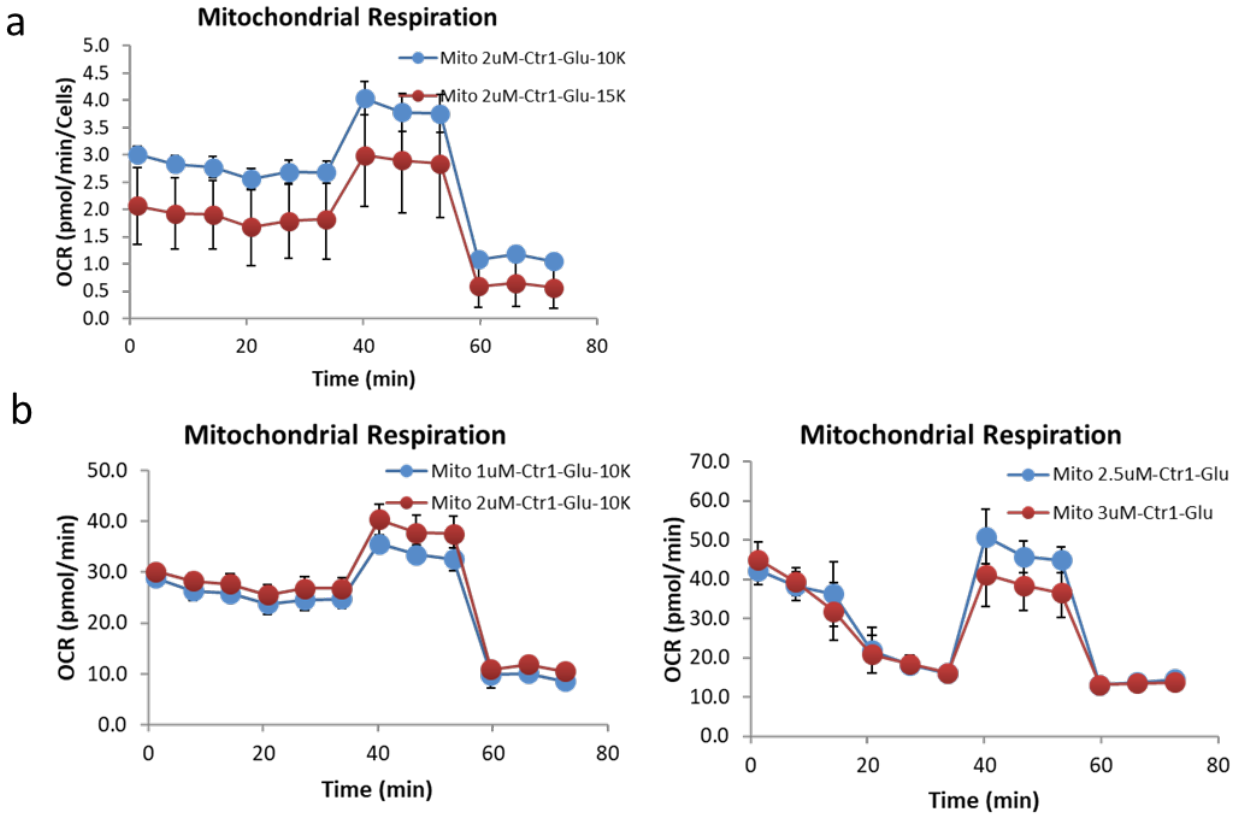

Figure 1: Optimization of cell number and FCCP concentration. (a) Seeding 10,000 cells/well gave better results (higher OCR) than 15,000 cells/well. (b) OCR was optimal after the addition of 2.5 µM FCCP.

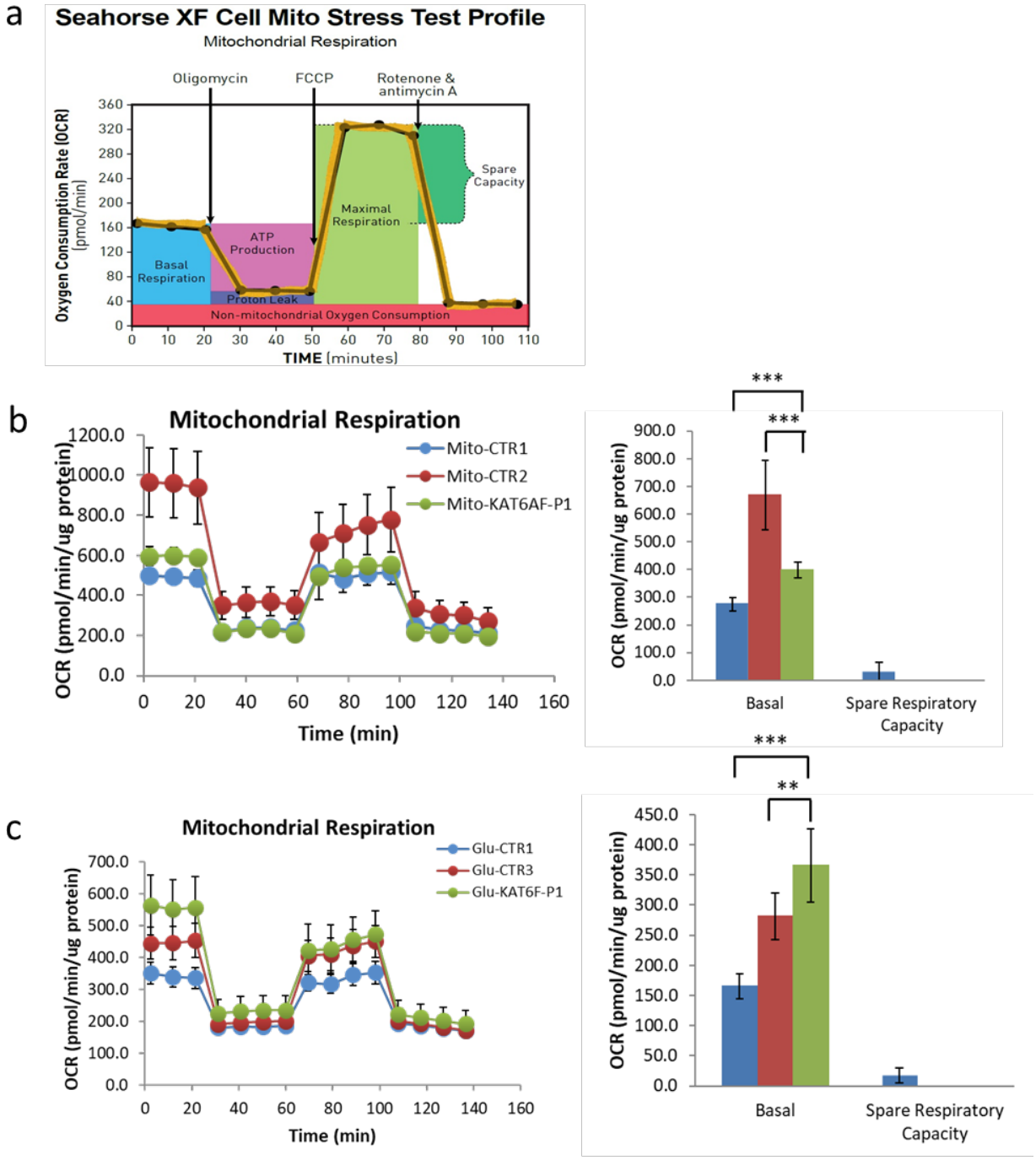

Figure 2: Respiratory flux profiles of KAT6A patient and control derived fibroblasts, as determined by a Seahorse Extracellular Flux Analyzer. (a) Illustrative respiratory flux profile indicating the edition of ATP synthase inhibitor oligomycin, electron transport chain uncoupler FCCP and complex I and III inhibitors rotenone and antimycin A. (b, c) OCR was measured

under basal conditions and after the sequential addition of oligomycin (7.5µM), FCCP (2.5µM) and antimycin A and rotenone (1.3µM). Quantitative analysis of basal OCR is shown. Resulting rates were normalized to protein concentration. ** indicates *P* value<0.01, *** indicates *P* value<0.001.

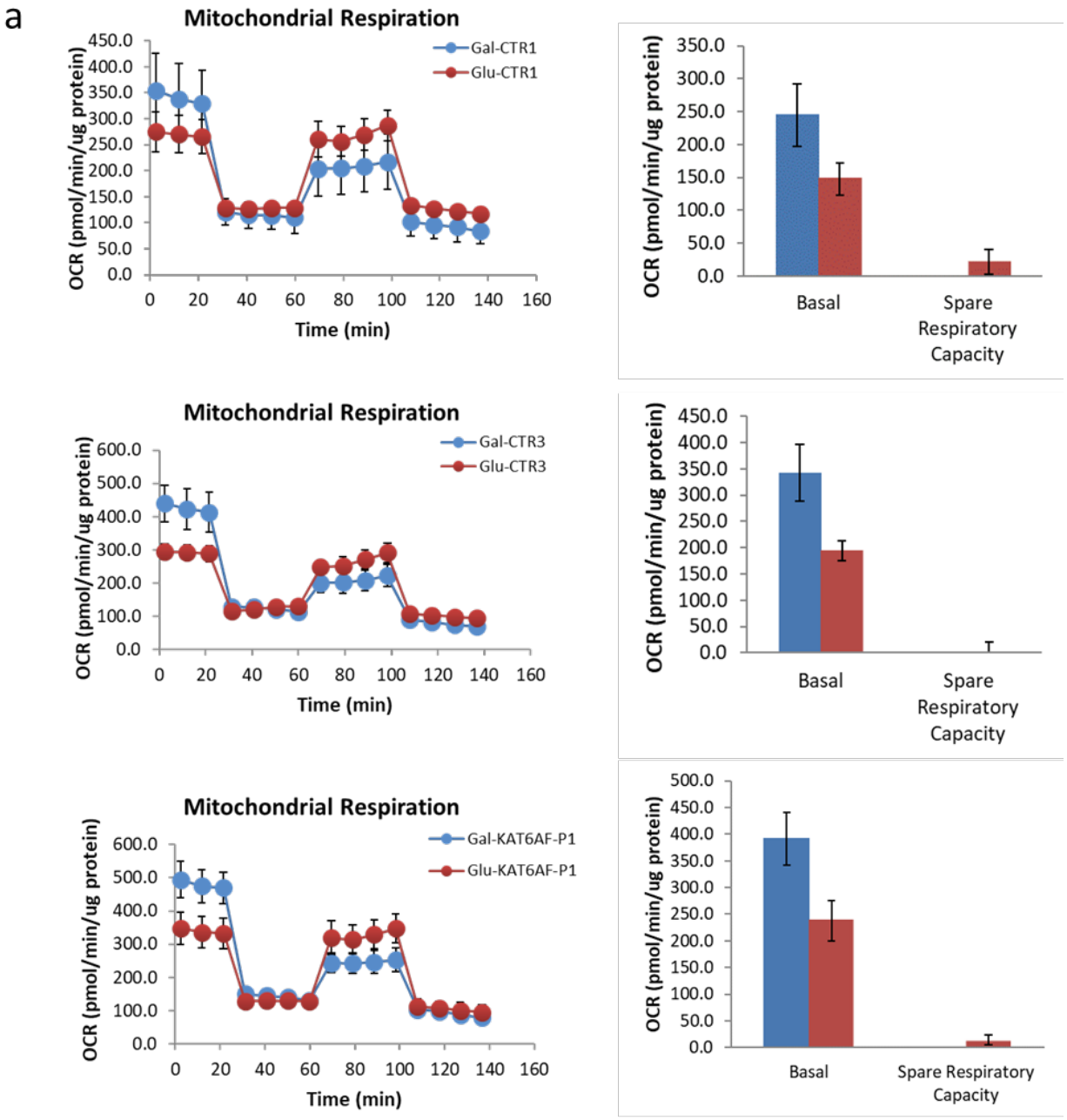

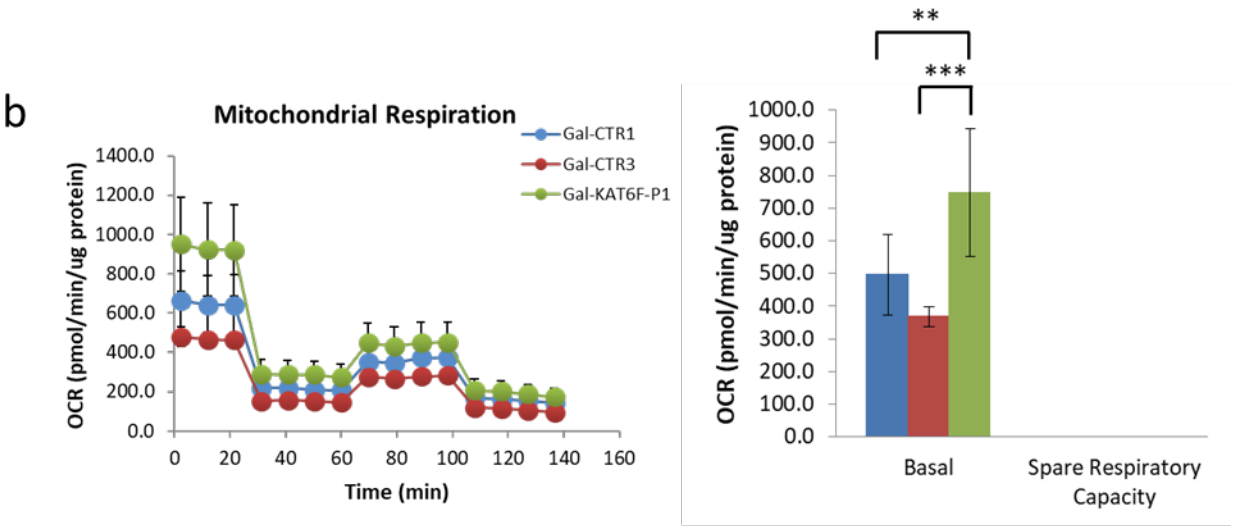

Figure 3. Respiratory flux profiles of KAT6A patient and control derived fibroblasts in galactose containing medium. OCR was measured under basal conditions and after the sequential addition of oligomycin, FCCP and antimycin A and rotenone. Quantitative analysis of basal OCR is shown. (a) Effect of galactose on OCR of control and patient's cells compared to glucose containing medium. (b) Patient's cells OCR compared to control cells in galactose containing medium. The experiment was repeated twice. Resulting rates were normalized to protein concentration. ** indicates *P* value<0.01, *** indicates *P* value<0.001.

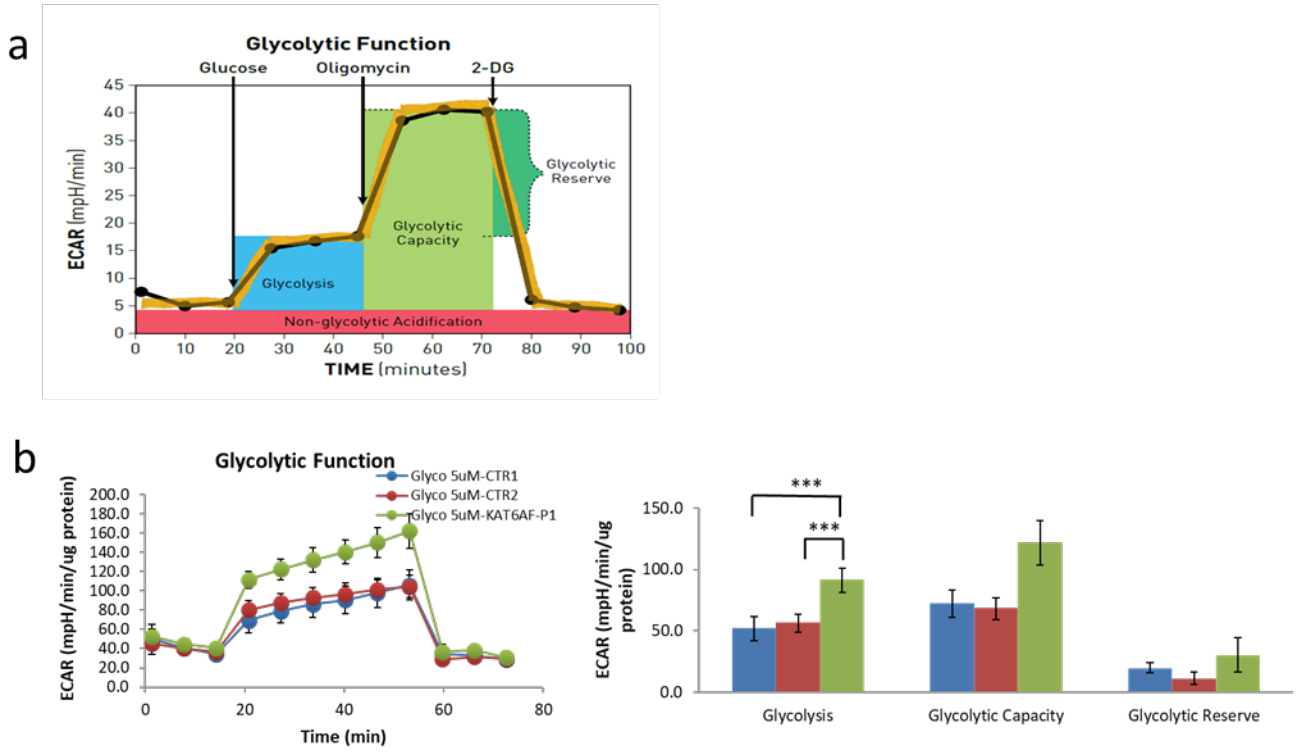

Figure 4. Glycolytic function in KAT6A patient and control derived fibroblasts, as determined by a Seahorse Extracellular Flux Analyzer. (a) Illustrative measurements of glycolysis, glycolytic capacity and glycolytic reserve after the addition of glucose, oligomycin and 2-DG. (b) ECAR was measured under basal conditions and after the addition of 10 mM glucose, 7.5µM oligomycin and 50 mM 2-DG. The experiment was repeated three times. Resulting rates were normalized to protein concentration. Quantitative analysis of glycolysis, glycolytic capacity and glycolytic reserve is shown. *** indicates *P* value<0.001.

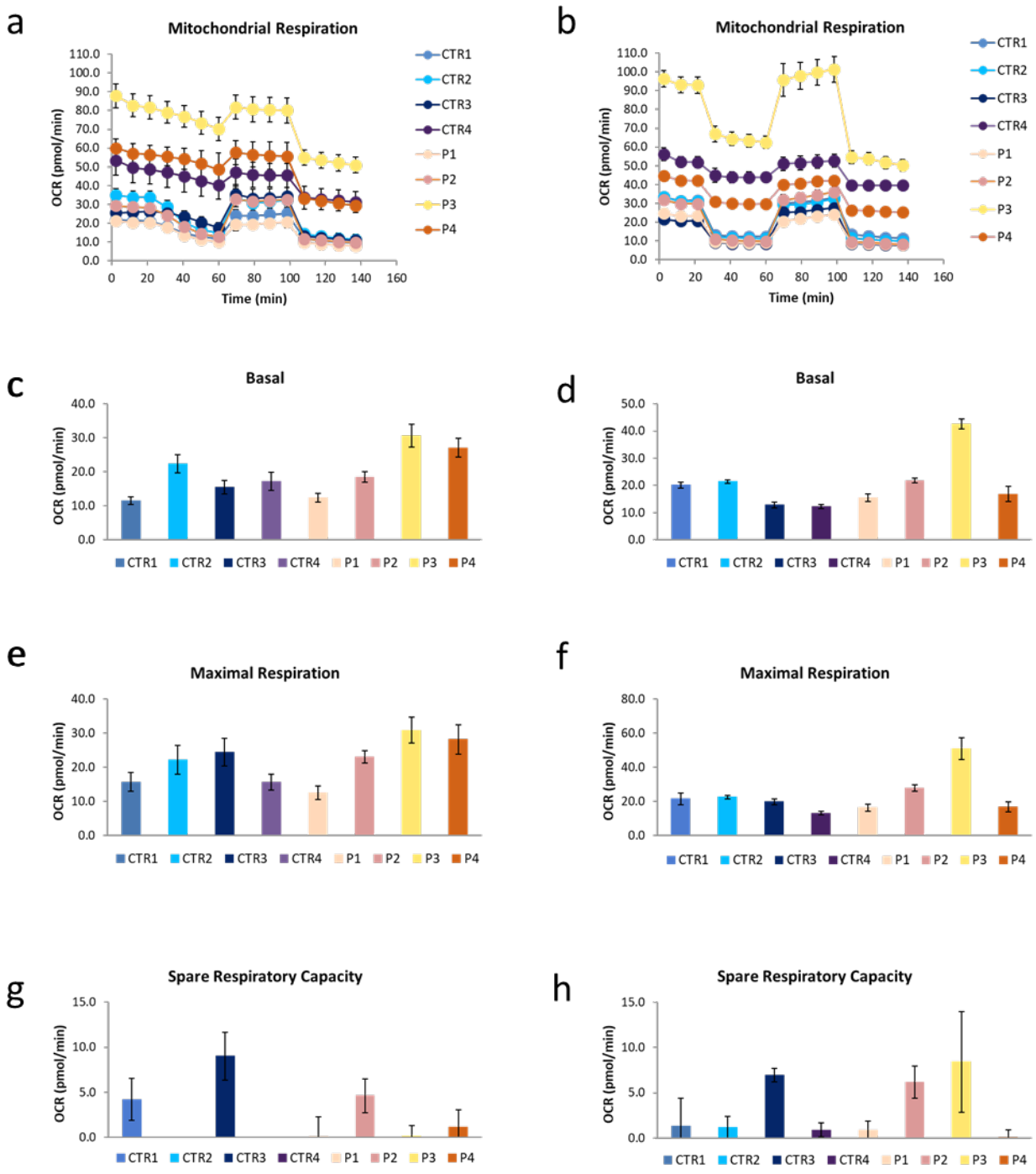

Figure 5. (a, b) Respiratory flux profiles of KAT6A patients (P1-4) and control (CTR1-4) derived fibroblasts, as determined by a Seahorse Extracellular Flux Analyzer. OCR was measured under basal conditions and after the sequential addition of oligomycin (5µM), FCCP (2.5µM) and antimycin A and rotenone (1µM). The experiment was repeated twice (a,b). (c, d)

Quantitative analysis of basal OCR. (e, f) Quantitative analysis of maximal respiration. (g, h) Spare respiratory capacity.

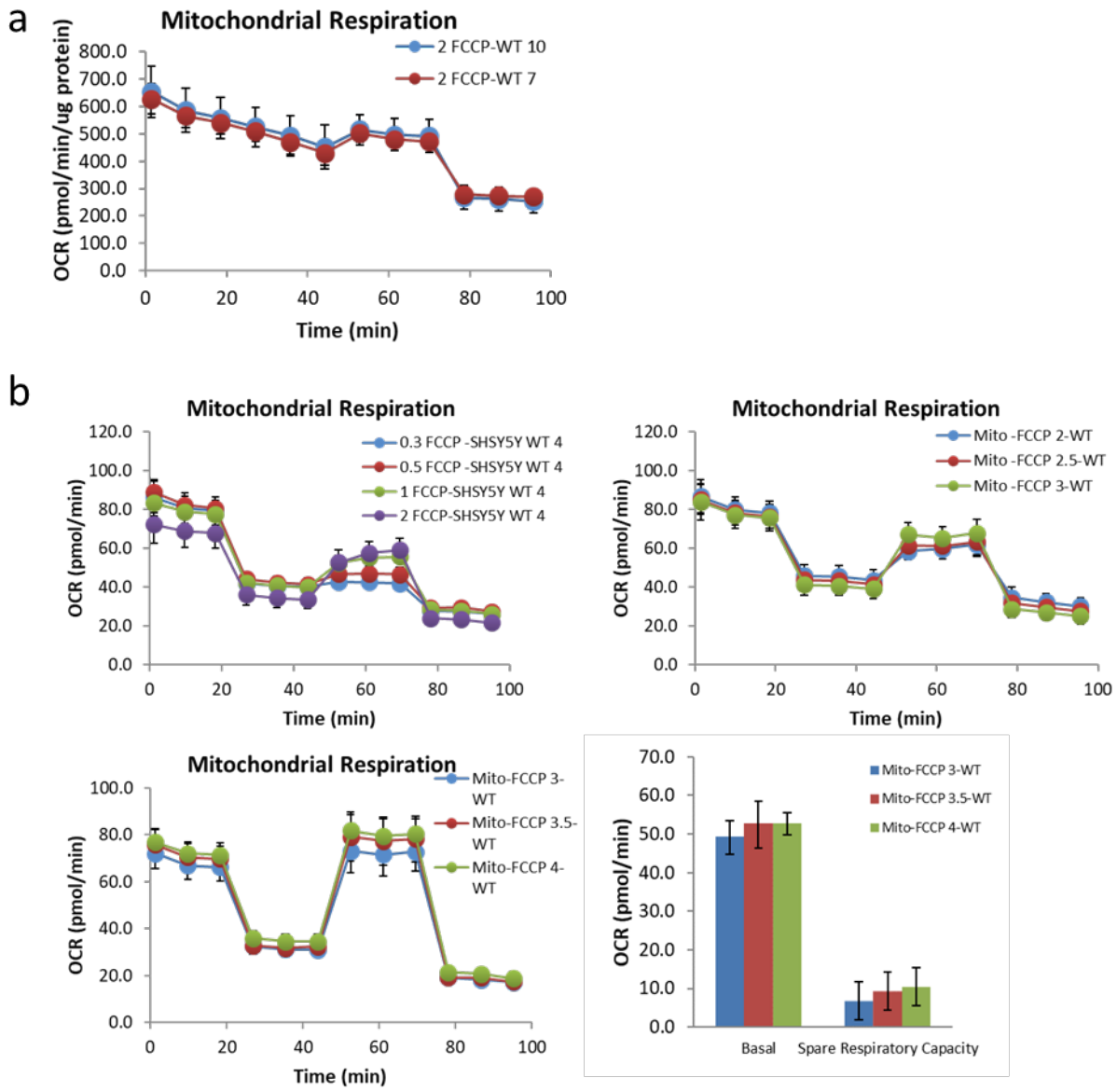

Figure 6: Optimization of SH-SY5Y cell number and FCCP concentration. (a) Seeding 7,000/10,000 cells/well gave the same results. (b) OCR after the addition of different concentrations of FCCP. Quantitative analysis of basal OCR for 3-4 µM FCCP is shown. OCR was optimal after the addition of 3.5/4 µM FCCP.

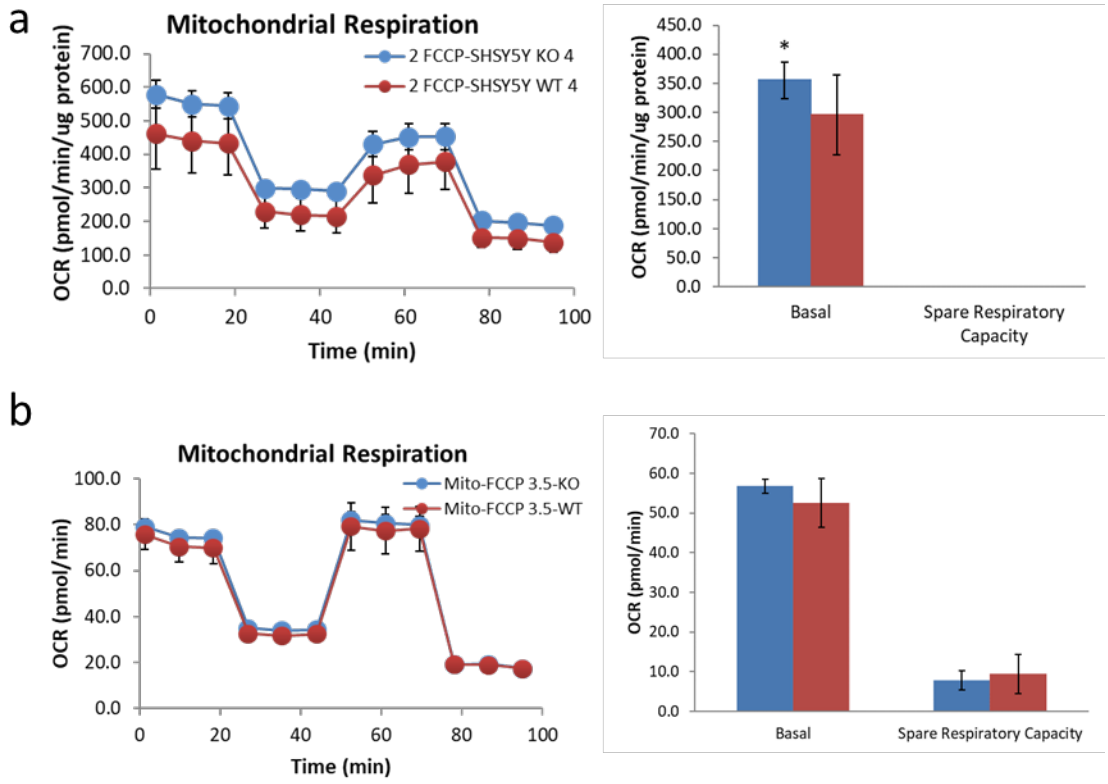

Figure 7: Respiratory flux profiles of SH-SY5Y WT cells and KAT6A KO cells, as determined by a Seahorse Extracellular Flux Analyzer. (a, b) OCR was measured under basal conditions and after the sequential addition of oligomycin (7.5µM), FCCP (2/3.5µM) and antimycin A and rotenone (1µM). Quantitative analysis of basal OCR is shown. * Indicates *P* value <0.05.

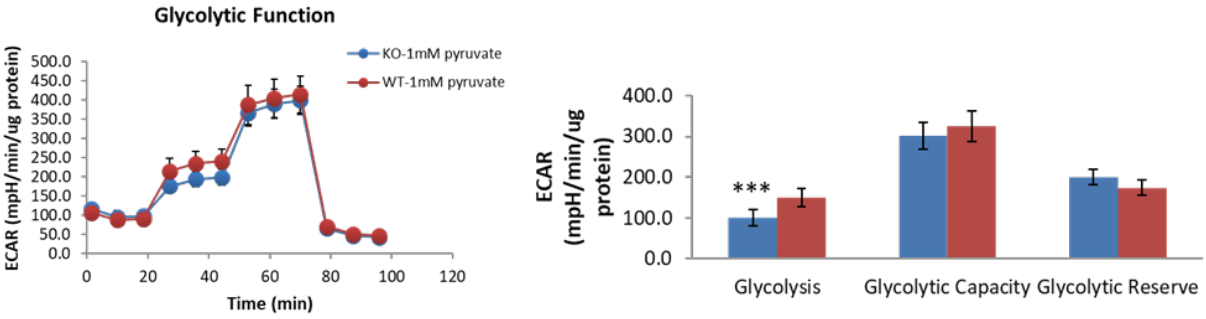

Figure 8: Glycolytic function of SH-SY5Y WT cells and KAT6A KO cells, as determined by a Seahorse Extracellular Flux Analyzer. ECAR was measured under basal conditions and after the

addition of 10 mM glucose, 7.5µM oligomycin and 100 mM 2-DG. The experiment was repeated three times. Resulting rates were normalized to protein concentration. Quantitative analysis of glycolysis, glycolytic capacity and glycolytic reserve is shown. *** indicates *P* value<0.001.

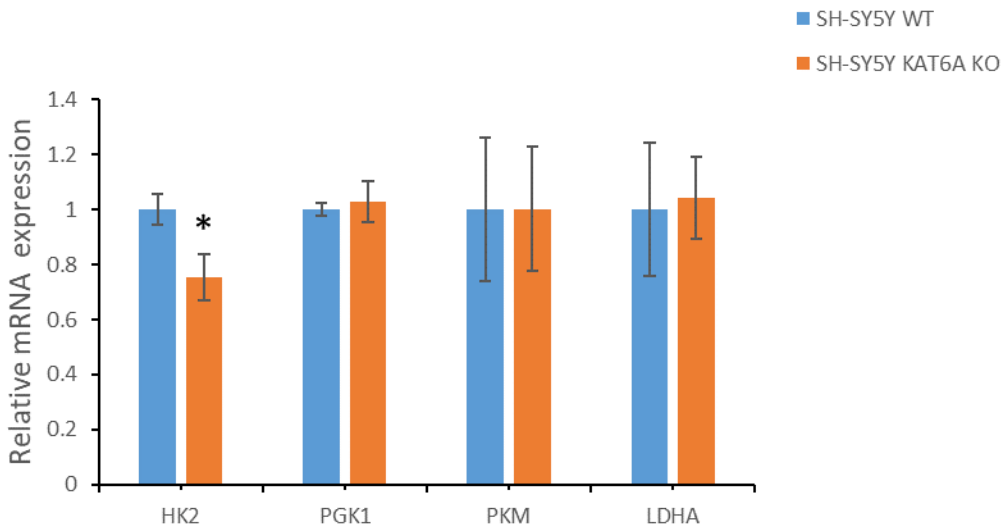

Figure 9: Real-time qPCR analysis shows mRNA expression levels of glycolytic genes in SH-SY5Y WT and SH-SY5Y KAT6A KO cells. *indicates *P* value < 0.05.

References:

Divakaruni, A.S., Paradyse, A., Ferrick, D.A., Murphy, A.N., Jastroch, M., 2014. Analysis and interpretation of microplate-based oxygen consumption and pH data, in: Methods in Enzymology. Academic Press, pp. 309–354. https://doi.org/10.1016/B978-0-12-801415-8.00016-3

Fu, J.Y., Huang, S.J., Wang, B.L., Yin, J.H., Chen, C.Y., Xu, J.B., Chen, Y.L., Xu, S., Dong, T., Zhou, H.N., Ma, X.Y., Pu, Y.P., Li, H., Yang, X.J., Xie, L.S., Wang, Z.J., Luo, Q., Shao, Y.X., Ye, L., Zong, Z.R., Wei, X. Di, Xiao, W.W., Niu, S.T., Liu, Y.M., Xu, H.P., Yu, C.Q., Duan, S.Z., Zheng, L.Y., 2024. Lysine acetyltransferase 6A maintains CD4+ T cell response via epigenetic reprogramming of glucose metabolism in autoimmunity. Cell

Metab. 36, 557-574.e10. https://doi.org/10.1016/j.cmet.2023.12.016

Hertig, D., Felser, A., Diserens, G., Kurth, S., Vermathen, P., Nuoffer, J.M., 2019. Selective galactose culture condition reveals distinct metabolic signatures in pyruvate dehydrogenase and complex I deficient human skin fibroblasts. Metabolomics 15, 32. https://doi.org/10.1007/s11306-019-1497-2

Russell, O.M., Gorman, G.S., Lightowlers, R.N., Turnbull, D.M., 2020. Mitochondrial Diseases: Hope for the Future. Cell 181, 168–188. https://doi.org/10.1016/J.CELL.2020.02.051

Wiesel-Motiuk, N., Assaraf, Y.G., 2020. The key roles of the lysine acetyltransferases KAT6A and KAT6B in physiology and pathology. Drug Resist. Updat. 53, 100729. https://doi.org/10.1016/j.drup.2020.100729